PROCEEDINGS, TOUGH Symposium 2006
Lawrence Berkeley National Laboratory, Berkeley, California, May 15–17, 2006

SHEAR-SLIP ANALYSIS IN MULTIPHASE FLUID-FLOW RESERVOIR ENGINEERING APPLICATIONS USING TOUGH-FLAC

Jonny Rutqvist, Jens Birkholzer, Frédéric Cappa, Curt Oldenburg, Chin-Fu Tsang

Lawrence Berkeley National Laboratory
Earth Sciences Division
Berkeley, CA, 94720, USA
e-mail: jrutqvist@lbl.gov

ABSTRACT

This paper describes and demonstrates the use of the coupled TOUGH-FLAC simulator for geomechanical shear-slip (failure) analysis in multiphase fluid-flow reservoir-engineering applications. Two approaches for analyzing shear-slip are described, one using continuum stress-strain analysis and another using discrete fault analysis. The use of shear-slip analysis in TOUGH-FLAC is demonstrated on application examples related to CO_2 sequestration and geothermal energy extraction. In the case of CO_2 sequestration, the shear-slip analysis is used to evaluate maximum sustainable CO_2-injection pressure under increasing reservoir pressure, whereas in the case of geothermal energy extraction, the shear-slip analysis is used to study induced seismicity during steam production under decreasing reservoir pressure and temperature.

INTRODUCTION

Major earthquakes, as well as induced seismicity during deep fluid injection or withdrawal, have long been associated with shear slip along discontinuities (Scholz, 1990). It has also been observed that fractures favorably oriented for slip, so-called critically stressed fractures, tend to be active ground water flow paths (e.g. Barton et al., 1995). If shear slip occurs on a critically stressed fracture, it can raise the permeability of the fracture through several mechanisms, including brecciation, surface roughness, and breakdown of seals (Barton et al., 1995). Thus, induced shear slip during reservoir-engineering operations such as underground CO_2 injection or geothermal energy extraction, may result in unwanted seismicity as well as substantial change in reservoir hydrological properties.

Analytical techniques for shear-slip analysis are commonly based on contemporary principal stress orientations with respect to pre-existing fault planes (e.g. Wiprut and Zoback, 2000; Streit and Hillis, 2004). The most fundamental criterion for fault (shear) slip is derived from the effective stress law and a Coulomb criterion, rewritten as:

$$\tau = C + \mu(\sigma_n - p) \qquad (1)$$

where τ is the shear stress, C is cohesion, μ is the coefficient of friction, σ_n is the normal stress, and p is the fluid pressure (Scholz, 1990). Equation (1) indicates that increasing fluid pressure during an underground injection (for example) may induce shear slip (Figure 1a).

Analytical techniques should be very useful for a first-order estimate of the potential for shear slip and for identification of the most critically oriented faults in a geological system. However, coupled reservoir-geomechanical simulations show that during underground fluid injection, the *in situ* stress field does not remain constant, but rather evolves in time and space, controlled by the evolutions of fluid pressure and temperature, and by site-specific structural geometry (Rutqvist and Tsang, 2005). Such poro-elastic and thermal-elastic stressing may change the *in situ* stress field in such a way that failure could be induced (Figure 1b).

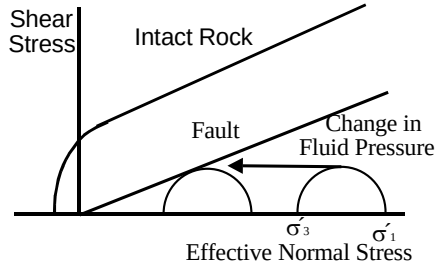

(a)

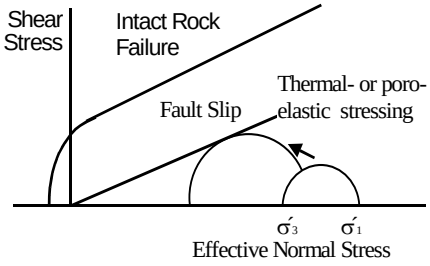

(b)

Figure 1. Shear slip along a pre-existing fault (or fracture) as a result of (a) increased fluid pressure and (b) thermal- or poro-elastic stressing

In this paper, we describe the use of the coupled reservoir-geomechanical simulator TOUGH-FLAC for evaluation of shear slip in geological systems. The TOUGH-FLAC simulator (Rutqvist et al., 2002; Rutqvist and Tsang, 2003) is based on the two established computer codes TOUGH2 (Pruess et al., 1999) and FLAC3D (Itasca, 1997). In linking these two codes, we can utilize the advanced multiphase fluid-flow capabilities in TOUGH2, as well as the advanced mechanical feature in FLAC3D, to perform shear-slip analysis in complex reservoir engineering applications. The approach is demonstrated for application examples related to CO_2 sequestration and geothermal energy extraction, but the approach presented here can also be used in many other types of applications.

SHEAR-SLIP ANALYSIS IN TOUGH-FLAC

In a TOUGH-FLAC simulation, shear-slip analysis can either be carried out as a continuum analysis, or discrete fault analysis. In a continuum analysis the potential for shear slip can be evaluated by studying the time evolution of the *in situ* stresses and assessing the potential for shear slip using a failure criterion. In the case of discrete fault analysis, both extent and magnitude of shear slip can be calculated using FLAC3D special fault mechanical elements.

Continuum Shear-Slip Analysis

A continuum shear-slip analysis may be conducted using the linear elastic option of FLAC3D. In such a case, the coupled TOUGH-FLAC simulation calculates changes in the stress field caused by changes in pressure and temperature. The evolution of the stress field can then be compared to a failure criterion to evaluate whether shear slip is likely not. For example, the evolution of stresses in a point may be compared to critical stresses obtained from the Coulomb criterion in Equation (1). In such a case, the orientation of a pre-existing fracture relative to the principal stresses must be known, to evaluate τ and σ_n for Equation (1). However, the location and orientation of fractures in the field may not be well known. It might therefore be useful, as a precaution, to assume that a fault (or pre-exiting fracture) could exist at any point with an arbitrary orientation. In such a case, the potential for shear slip can be evaluated with a Coulomb failure criterion in the following form (Jaeger and Cook, 1979):

$$|\tau_{m2}| = (\sigma_{m2} - P_{sc})\sin\varphi + S_0\cos\varphi \qquad (2)$$

where τ_{m2} and σ_{m2} are the two-dimensional maximum shear stress and mean stress in the principal stress plane (σ_1, σ_3), defined as:

$$\tau_{m2} = \frac{1}{2}(\sigma_1 - \sigma_3) \qquad (3)$$

$$\sigma_{m2} = \frac{1}{2}(\sigma_1 + \sigma_3) \qquad (4)$$

where S_0 and φ are the coefficient of internal cohesion and angle of internal friction of the fault, respectively.

This can also be expressed in terms of effective principal stresses as:

$$\sigma'_1 = C_0 + q\sigma'_3 \qquad (5)$$

where C_0 is the uniaxial compressive strength and q is the slope of the σ'_1 versus σ'_3 line, which is related to μ according to:

$$q = \left[\left(\mu^2 + 1\right)^{\frac{1}{2}} + \mu\right]^2 \qquad (6)$$

In the examples shown in this paper, the potential for shear slip is estimated using zero cohesion ($S_0 = 0$) and a friction angle of 30°, leading to the following criterion for shear slip:

$$\sigma'_1 = 3\sigma'_3 \qquad (7)$$

Thus, shear slip would be induced whenever the maximum principal effective stress exceeds three times the minimum compressive effective stress.

A zero cohesion and a friction angle of 30° correspond to a static coefficient of friction $\mu_s = \tan 30° \approx 0.6$, which is a lower-limit value frequently observed in studies of the correlation between hydraulic conducting fractures and maximum shear stress in fractured rock masses (e.g.. Barton et al., 1995).

Shear-Slip Analysis Along Discrete Faults

In general, the mechanical behavior of faults and fault zones can be represented in FLAC^{3D} by special mechanical interfaces (Figure 2a), by an equivalent continuum representation using solid elements (Figure 2b), or by a combination of mechanical interfaces and solid elements. Multiple element representation might be necessary to represent complex, heterogeneous permeability structures in major fault zones. This might include a low-permeability fault core and adjacent damaged rock zones.

Figure 2a shows a fault represented by the FLAC^{3D} mechanical interface. An interface can be used to model the mechanical behavior of faults characterized by Coulomb sliding and/or separation. Interfaces have the properties of friction, cohesion, dilation, normal and shear stiffness, and tensile strength. An interface element representation is perhaps the most appropriate if the thickness of the fault is negligible compared to the size of the problem. This may include major fault zones in a regional-scale model (on the order of kilometers), or in the case of minor, single-shear fractures at a smaller scale. To simulate permeability enhancement

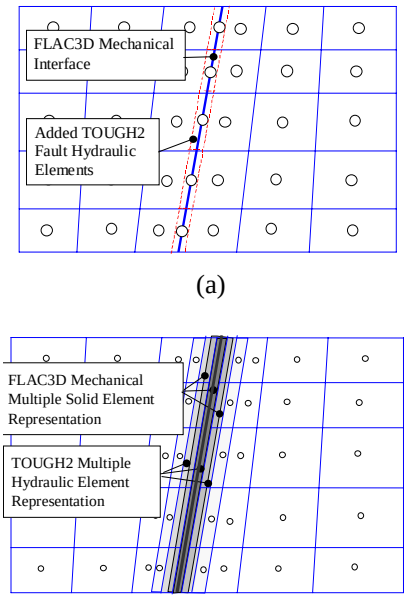

Figure 2. Fault plane representation in linked TOUGH2 and FLAC3D analysis using (a) FLAC3D mechanical interface, or (b) multiple solid elements with anisotropic properties.

along the interface, or sealing effects across the interface, TOUGH2 hydraulic elements must be added along the interface. The TOUGH2 hydraulic element is necessary to provide fluid pressure that will act within the fault, affecting the effective normal stress, which in turn affects the shear strength through the Coulomb criterion.

An alternative approach to the interface element is to represent the fault as an equivalent continuum using FLAC^{3D} standard solid elements (Figure 2b). In an equivalent continuum model representation of a fault structure, the fault mechanical properties can be represented by constitutive models of various sophistication, from the simplest isotropic linear elastic to more complex elasto-plastic or visco-plastic (creep) models. One particularly useful approach, available in FLAC^{3D}, is to represent the mechanical behavior of the fault as a ubiquitously fractured media. Such a model can be used to represent strongly anisotropic mechanical behavior, including anisotropic plasticity.

The use of interface elements for fault representation in TOUGH-FLAC was demonstrated by Rutqvist and Tsang (2005). However, it is generally more difficult to generate the required gridding in FLAC3D and TOUGH2, and the hydromechanical coupling of FLAC3D interface behavior to TOUGH2 is more complicated. Therefore, if fault mechanical behavior can be appropriately represented with solid elements, the hydromechanical coupling between FLAC3D and TOUGH2 is more straightforward to implement.

ESTIMATING MAXIMUM SUSTAINABLE PRESSURE DURING CO_2 INJECTION

Caprock integrity and reservoir leakage is a key issue for both short- and long-term performance of geological CO_2 storage. In the short term, leakage is an important safety issue during active CO_2 injection. In the long term, leakage impacts the sequestration effectiveness of the once-injected CO_2. A coupled reservoir-geomechanical analysis of a CO_2 injection operation can be used to estimate the maximum sustainable injection pressure, which is an injection pressure that will not result in unwanted damage such as fault reactivation or fracturing. A shear-slip analysis can be used to estimate where, when, and what type of shear slip could occur. In the next two subsections, we demonstrate the use of TOUGH-FLAC for evaluation of maximum sustainable injection pressure using continuum shear-slip analysis and shear-slip analysis with discrete fault representation.

Continuum Shear-Slip Analysis

In this simulation example, compressed CO_2 is injected at 1,500 m depth into a permeable formation overlaid by low-permeability caprock (Figure 3). (Details of material properties and input data are given in Rutqvist and Tsang, 2005). We simulate a constant-rate CO_2 injection, evaluating the maximum sustainable injection pressure for two different stress regimes: (1) a compressional stress regime with $S_H = 1.5 \times S_V$, and (2) an extensional stress regime with $S_H = 0.7 \times S_V$. The maximum sustainable injection pressure could also be estimated analytically, using Equations (2) or (5) for lithostatic vertical stress, S_V = 33.2 MPa, at 1.500 meters. The analytical estimate of the maximum sustainable injection pressure from initial (undisturbed) stresses would be 25 MPa for a compressional stress regime and 18 MPa for an extensional stress regime. We will compare these values to our coupled reservoir-geomechanical simulation results at the end of this section.

Figure 4 presents vertical profiles of several key parameters after 3 years of injection. At this time, the injection pressure has reached 27 MPa, which is about 80% of the lithostatic stress (Figure 4a). At this time, the CO_2 is completely contained within the injection zone (Figure 4b). However, the increased fluid pressure within the injection zone and the overlying caprock induces changes in horizontal and vertical effective stresses, according to:

$$\Delta\sigma'_x = \Delta\sigma_x - \Delta P \quad (8)$$

$$\Delta\sigma'_z = \Delta\sigma_z - \Delta P \quad (9)$$

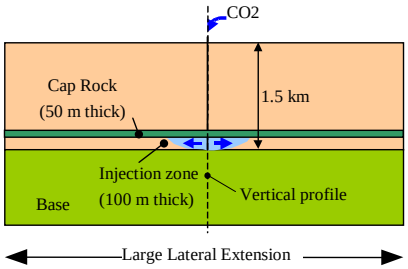

Figure 3. Schematic of model geometry for modeling of CO_2 injection and continuum shear-slip

Figure 4c and d shows that both effective and total (confining) stresses change with the changed reservoir pressure. Increases in total stresses are caused by poro-elastic expansion, which is partly restricted by the stiffness of the surrounding rock-mass structure. In general, effective stress changes much more in the vertical direction as a result of the free-moving groundsurface (Rutqvist and Tsang, 2005).

Changes in the stress field shown in Figure 4c and d should be added to the initial pre-injection *in situ* stresses to obtain the stress field after 3 years of injection. However, the three-dimensional pre-injection *in situ* stress field may not be entirely known. Therefore it is useful to evaluate the maximum sustainable injection pressure for various *in situ* stress regimes, including compressional pressure regime (for which $S_H > S_V$) and extensional regime (for which $S_H < S_V$).

Figure 4e and f present vertical profiles for evaluation of shear-slip potential for the two different stress regimes. In the case of a compressional stress regime (Figure 4e), shear slip could occur in the lower part of the cap, at the interface with the injection zone, as well as at the lower part of the injection zone. However, the shear slip could probably not propagate through the upper part of the cap, which would remain intact. In the case of an extensional stress regime, shear slip might first be induced near the groundsurface and in the overburden rock above the zone of pressure increase. Thereafter, shear slip might also be induced in the caprock, just above the injection zone.

In Figure 5, the path of the principal effective stresses, σ'_1 and σ'_3, in the lower part of the caprock (near its interface with the injection zone) is plotted and compared to the failure criterion in Equation (7). For a compressional stress field, the principal stresses would move into a region of likely shear slip after just over one year of injection at an injection pressure of about 24 MPa. In an extensional stress regime, shear slip could occur just after three years of injection at an injection pressure of about 28 MPa.

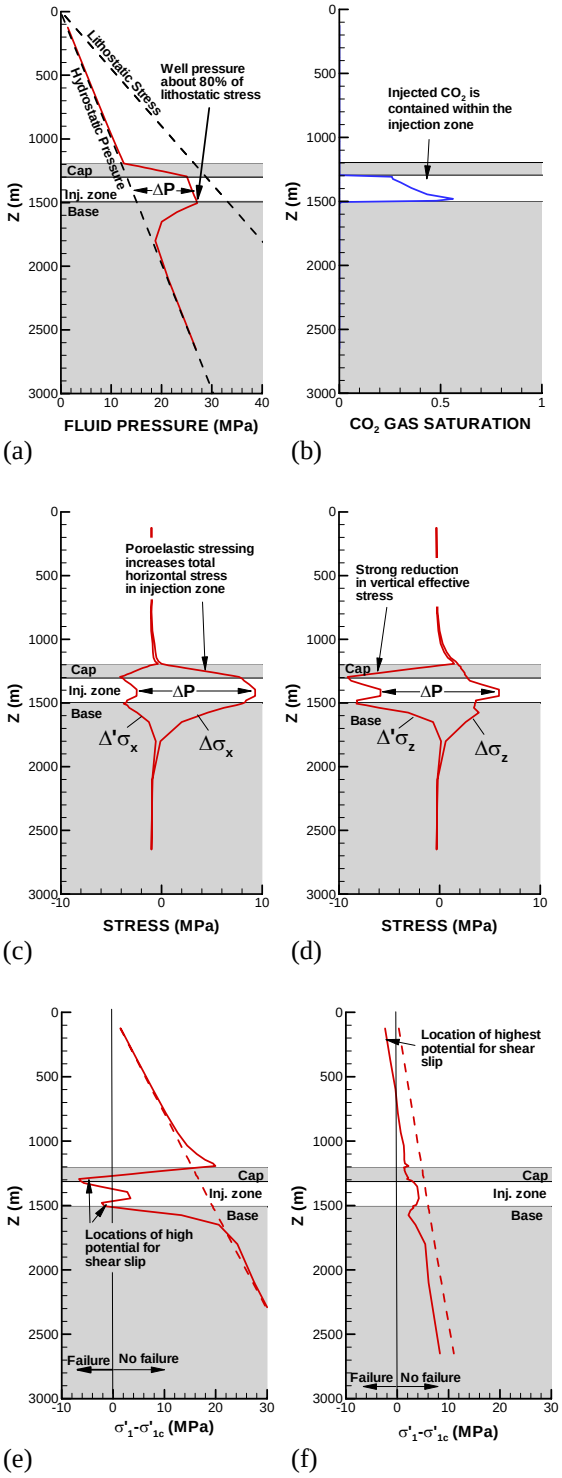

Figure 4. Vertical profiles of (a) fluid pressure, (b) CO_2 saturation, (c) change in horizontal effective and total stress, (d) change in vertical effective and total stress, (e and f) $\sigma'_1 - \sigma'_{1c} = \sigma'_1 - 3\sigma'_3$ for compressional and extensional stress regimes, respectively.

Thus, in this case the maximum sustainable injection pressure would be estimated as 24 and 28 MPa, for the compressional and extenstional stress regimes, respectively. The analytical estimates calculated at the beginning of this section were respectively 25 and 18 MPa, indicating that the analytical estimate for the extensional stress regime might be overly conservative.

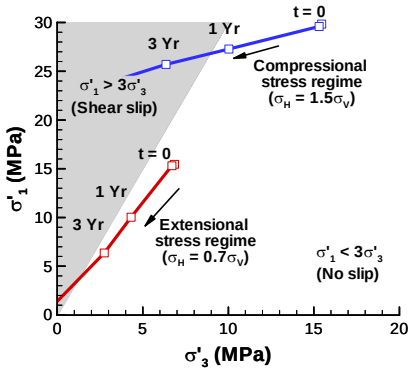

Figure 5. Principal (effective) stress path at the bottom of the caprock for compressional and extensional stress regimes

Shear-Slip Analysis with a Discrete Fault

In this simulation example, a shear-slip analysis is conducted using a discrete fault representation in TOUGH-FLAC. As in the previous example, compressed CO_2 is injected at 1,500 m depth into a permeable formation overlaid by a low-permeability caprock. However, in this case the injection zone is effectively bounded by an offset fault (Figure 6). In this example, an extensional stress regime with $S_H = 0.7 \times S_V$ is assumed, and the fault is considered cohesiveless, with a friction angle of 25°.

In this case we can also estimate the maximum sustainable injection pressure using Equation (1), for the undisturbed initial stress field. At the depth of the injection, the initial stresses are S_V = 33 MPa, and $S_H = 0.7 \times S_V$ = 23 MPa. Using Equation (1) and considering the fault angle for estimation of τ and σ_n, we estimate the maximum sustainable injection pressure to P = 19.8 MPa. At the end of this section, we will compare this number to the results of our TOUGH-FLAC shear-slip analysis.

In the TOUGH-FLAC simulation, the fault is discretized into solid elements with anisotropy of mechanical (elasto-plastic) and hydrologic properties. In this model, fault permeability changes with shear such that for a fully reactivated fault (maximum shear strain), permeability increases by two orders of magnitude. This is simulated by relating the permeability changes to maximum shear strain, ε_{sh}, according to:

$$\frac{k}{k_0} = 1 + \beta \cdot \Delta\varepsilon_{sh} \qquad (10)$$

where β is set to 1×10^{-4} to obtain a two-order-of-magnitude permeability increase for a fully reactivated fault. Other material properties and input data are similar to that of the above continuum shear-slip analysis, which can be found in Rutqvist and Tsang (2005).

Figure 7 shows the evolution of injection pressure during the constant-rate CO_2 injection. In Figure 7, the fully coupled hydromechanical simulation (solid line in Figure 7) is compared to an uncoupled simulation with no fault reactivation (dashed line in Figure 7). If no fault reactivation is considered, fluid pressure would quickly rise above lithostatic stress. On the other hand, if fault reactivation and shear-induced permeability changes are considered, the injection pressure does not rise as high, but peaks at a magnitude well below lithostatic stress. Limited shear slip and change in permeability begin at an injection pressure of about 19 MPa, but shear slip does not propagate across the upper cap until an injection pressure of about 25 MPa.

Figure 8 shows that after 6 months, the zone of shear slip, observed as a zone of localized substantial shear strain, extends all the way through the upper cap. Thus, a new flow path has opened up across the upper cap. As a result, the injected CO_2-rich fluid reaches and migrates up along the fault after about 1 year and 4 months (Figure 9).

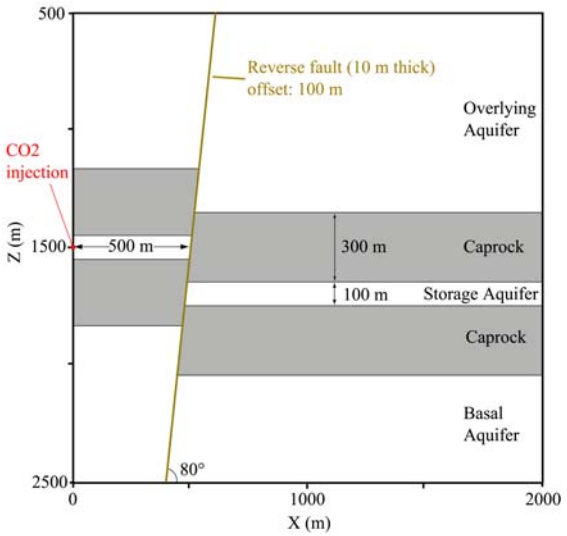

Figure 6. Model for TOUGH-FLAC modeling of discrete fault hydromechanical behavior during CO_2 injection

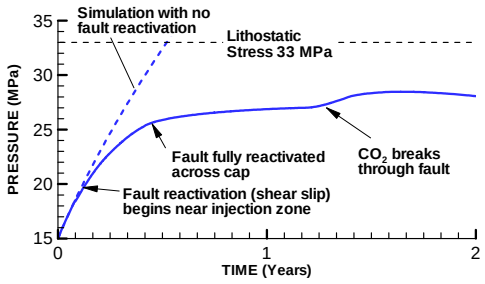

Figure 7. Simulated evolution of injection pressure with and without consideration of shear-slip-induced fault permeability changes

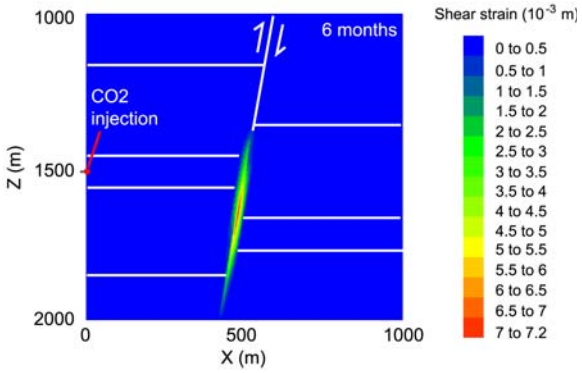

Figure 8. Contour of maximum shear strain after 6 months of injection

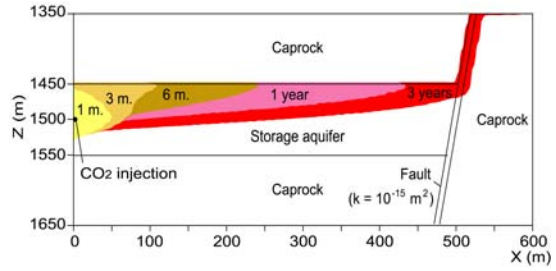

Figure 9. Simulated evolution of CO_2-rich phase

The maximum sustainable injection pressure in this case is between 19 to 25 MPa. At 19 MPa, the shear-slip induced permeability changes in the fault affect the injection pressure by leakage into the underlying formation. Upward leakage to overlying formations does not occur until the fault slip has propagated through the upper cap, which occurs at an injection pressure of about 25 MPa. Thus, in this case the simplified analytical estimate of the sustainable injection pressure (19.8 MPa) appears to be conservative.

INDUCED SEISMICITY DURING GEOTHERMAL STEAM PRODUCTION

Seismicity induced by underground injection or fluid withdrawal—e.g., during oil and gas, or geothermal energy extraction—may be of concern to local communities. One example is The Geysers geothermal field, California, where at least some of the felt earthquakes have been related to the geothermal energy production activities (Oppenheimer, 1986). Therefore, as part of project for the California Energy Commission, coupled thermal-hydrological-mechanical (THM) simulations with TOUGH-FLAC are conducted to investigate the relative contributions of different mechanisms that may be causing induced seismicity at The Geysers (Rutqvist et al., 2006).

The first part of this study includes a coupled THM analysis of reservoir-wide steam production over three decades (Rutqvist et al., 2006). The first analysis was conducted on a cross-axis (NE-SW) two-dimensional model grid of the Geysers Geothermal Field (Figure 10). The TOUGH2 part of the TOUGH-FLAC analysis was simulated with equation of state module EOS3 to run a steady natural-state simulation followed by a 35-year steam production simulation.

Similarly to the previous example of CO_2 sequestration, we analyzed the potential for shear slip by comparing the evolution of the effective principal stress to that of the failure criterion in Equation (7). However, previous studies at the Geysers (e.g. Lockner et al., 1982; Oppenheimer, 1986) indicated that shear stress in the region is probably near the rock-mass frictional strengths and that a very small perturbation of the stress field could trigger seismicity. Therefore, assuming that the initial principal stress state is on the verge of failure, we analyzed changes in the effective principal stress state and evaluated whether the stress state moves toward failure or away from failure.

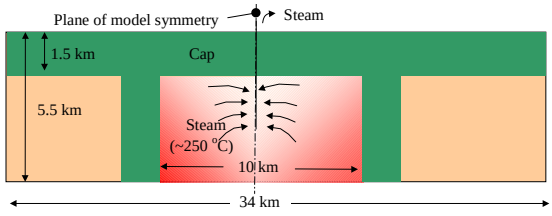

Figure 10. Schematic of model geometry for coupled THM modeling of steam production at the Geysers Geothermal Field (symmetry condition marked with the plane of symmetry was used enabling with the left hand side in the calculation grid)

Figure 11 presents vertical profiles of simulation results at the center of the geothermal reservoir. The simulation broadly models the pressure and temperature decline that has been observed at the Geysers (e.g., Williams, 1992). During the simulated 35-year constant steam production, the reservoir pressure declines by a few MPa, and the reservoir temperature cools a few degrees (Figure 11a and b).

Figure 11c and d show that changes in the stress field are on the order of 1 MPa over the 35-year production period. There is an increase in horizontal stress in the caprock, whereas both vertical and horizontal effective stresses increase within the reservoir. Changes on the order of 1 MPa, over 35 years appear to be very small. However, as discussed above, the initial principal stress state is likely on the verge of failure, and therefore only a very small stress perturbation might induce seismicity. This hypothesis is supported by recent studies of remotely triggered seismicity at the Geysers, which indicates that seismic events can be triggered by a stress change as low as 0.03 to 0.07 MPa (Prejean et al., 2004). Thus, a 1 MPa stress change should be sufficient to induce repeated triggering of small seismic events.

Figure 11e and f presents the maximum principal stress minus the critical maximum principal stress ($\Delta\sigma'_1 - \Delta\sigma'_{1c} = \Delta\sigma'_1 - 3\Delta\sigma'_3$) for two different stress regimes: (1) a compressional stress regime with $S_H > S_V$, and (2) an extensional stress regime with $S_H < S_V$. The figures indicate that at 35 years, shear slip (and induced seismicity) would be likely in the caprock, but only in the case of a compressional stress regime. For an extensional stress regime, on the other hand, shear slip appears to be unlikely, both in the reservoir and in the caprock.

Figure 12 presents the stress path at a point located in the caprock, 750 meter below ground surface. The figure shows that if the maximum principal *in situ* stress is horizontal (compressional stress regime), the state of principal effective stress (σ'_1, σ'_3) continuously moves into the zone of failure (solid line in Figure 12). On the other hand, if the major principal stress is vertical (extensional stress regime), the principal stress state moves away from the zone of failure (dashed line in Figure 12). This indicates that seismicity could be continuously induced over the 35-year production period, but only if the major principal stress is horizontal (compressional stress regime).

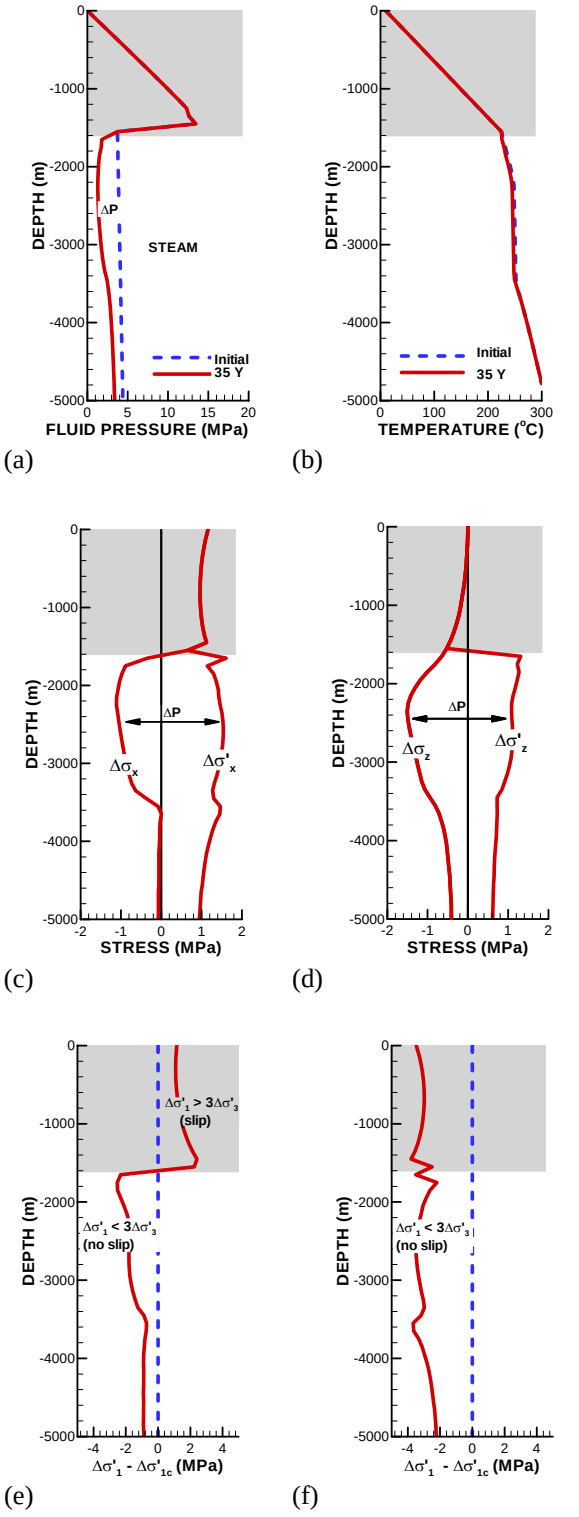

Figure 11. Vertical profiles of (a) fluid pressure, (b) temperature, (c) changes in horizontal effective and total stress, (d) changes in vertical effective and total stress, (e and f) $\Delta\sigma'_1 - \Delta\sigma'_{1c} = \Delta\sigma'_1 - 3\Delta\sigma'_3$ for compressional and extensional stress regimes, respectively

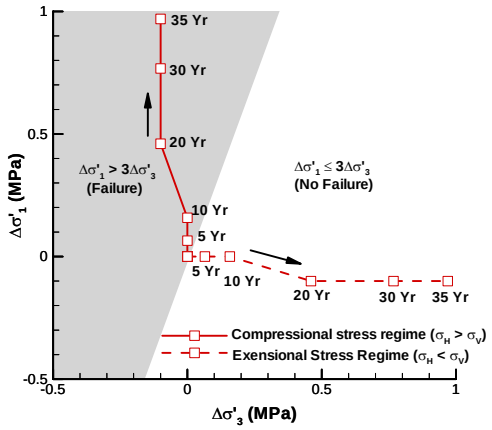

Figure 12. Path of effective stress changes ($\Delta\sigma'_1$, $\Delta\sigma'_3$) within the caprock at a depth of –750 meters

The results obtained by this TOUGH-FLAC analysis are in agreement with observations of induced seismicity and its correlation to steam production at The Geysers (Rutqvist et al., 2006). Earlier attempts to study the mechanisms of induced seismicity at The Geysers have been based on analyses of seismic signatures, correlations between production data seismicity, and analytical poro-elastic or thermo-elastic solutions of steam production. A coupled reservoir-geomechanical analysis with TOUGH-FLAC cannot only be used to study induced seismicity for the past production history, but might also be used for optimization of future production, while minimizing induced seismicity.

CONCLUDING REMARKS

In this paper, we describe and demonstrate the use of TOUGH-FLAC for geomechanical fault-slip analysis in multiphase fluid-flow reservoir engineering applications. The main advantage of this approach (compared to more conventional analytical methods) is that the coupled numerical analysis takes into account changes in the stress field induced by the injection or withdrawal of fluid. Using the coupled reservoir-geomechanical numerical analysis, the shear-slip analysis can be fully integrated with the multiphase fluid-flow reservoir analysis of a site, and can therefore be used for design and optimization of injection/withdrawal operations. This would include optimization of injected CO_2 mass, while minimizing the risk for leakage, or optimizing geothermal steam production, while minimizing induced seismicity.

ACKNOWLEDGMENT

The work presented in this paper was financed by contributions from the California Energy Commission (CEC), the Ministry of Economy, Trade and Industry Ministry (METI) of Japan, and the US Environmental Protection Agency, Office of Water and Office of Air and Radiation, under an Interagency Agreement with the U.S. Department of Energy at the Lawrence Berkeley National Laboratory, No. DE-AC02-05CH11231.

REFERENCES

Barton, C. A., M. D. Zoback and D Moos, Fluid flow along potentially active faults in crystalline rock. *Geology*, 23, 683–686, 1995.

Itasca Consulting Group, *FLAC 3D, Fast Lagrangian Analysis of Continua in 3 Dimensions. Version 2.0.* Five volumes. Minneapolis, Minnesota, Itasca Consulting Group, 1997.

Jaeger, J. C. and N. G. W. Cook, *Fundamentals of Rock Mechanics.* Chapman and Hall, London. 1979.

Lockner, D.A., R. Summer, D. Moore, and J.D. Byerlee. Laboratory measurements of reservoir rock from the Geysers Geothermal Field, California. *Int. J. Rock mech. Min. Sci.*, 19, 65–80, 1982.

Oppenheimer, D.C., Extensional tectonics at the Geysers Geothermal Area, California, *J. Geophys. Res.*, 91,11463–11476, 1986.

Prejean, S.G., D. P. Hill, E. E. Brodsky, S.E. Hough, M. J. S. Johnston, S. D. Malone, D. H Oppenheimer, A. M. Pitt , and K. B. Richards-Dinger 2004. Bulletin of Seismological Society of America, 94(6B),S348-S356, 2004.

Pruess, K., C. Oldenburg, and G. Moridis, *TOUGH2 User's Guide, Version 2.0*, Report LBNL-43134, Lawrence Berkeley National Laboratory, Berkeley, Calif., 1999.

Rutqvist, J., and C.-F. Tsang, TOUGH-FLAC: A numerical simulator for analysis of coupled thremal-hydrologic-mechanical processes in fractured and porous geological media under multi-phase flow conditions. Proceedings of the TOUGH symposium 2003, Lawrence Berkeley National Laboratory, Berkeley, May 12–14, 2003.

Rutqvist, J. and C.-F. Tsang. Coupled hydromechanical effects of CO_2 injection. In: Tsang C.F., Apps J.A., editors. *Underground Injection Science and Technology*. Elsevier, p. 649–679, 2005.

Rutqvist, J., Y.-S. Wu, C.-F. Tsang and G. Bodvarsson, A modeling approach for analysis of coupled multiphase fluid flow, heat transfer, and deformation in fractured porous rock. *Int. J. Rock Mech. Min. Sc.i.* 39, 429–442, 2002.

Rutqvist, J., E. Majer, C. Oldenburg, J. Peterson, and D. Vasco. Integrated modeling and field study of potential mechanisms for induced seismicity at the Geysers geothermal field, California. Submitted to Geothermal Research Council, Annual Meeting, 2006.

Scholz, C. H., *The Mechanics of Earthquakes and Faulting.* Cambridge University Press, New York., 1990.

Streit, J.E., and R. R. Hillis, Estimating fault stability and sustainable fluid pressures for underground storage of CO_2 in porous rock. Energy, 29, 1445–1456, 2004.

Wiprut, D., and M.D. Zoback, Fault reactivation and fluid flow along a previous dominant fault in the northern North Sea. *Geology*, 28, 595–598, 2000.

Williams K.H. Development of a reservoir model for The Gyesers geothermal field. In Monograph on The Geusers Gepthartmla Field , Spcial Report no. 19, Gotheraml Recources Councel, ed. C. Stone, 179-186. Geothermal Research Council, 1992.